

Computer simulation of ionic conduction in $\text{ZrF}_4\text{-BaF}_2$ glass: II. Normal-mode analysis

This article has been downloaded from IOPscience. Please scroll down to see the full text article.

1997 J. Phys.: Condens. Matter 9 5157

(<http://iopscience.iop.org/0953-8984/9/24/014>)

View [the table of contents for this issue](#), or go to the [journal homepage](#) for more

Download details:

IP Address: 171.66.16.207

The article was downloaded on 14/05/2010 at 08:57

Please note that [terms and conditions apply](#).

Computer simulation of ionic conduction in $\text{ZrF}_4\text{--BaF}_2$ glass: II. Normal-mode analysis

R Yamamoto[†], M Kano[‡] and Y Kawamoto[‡]

[†] Department of Physics, Kyoto University, Kyoto 606-01, Japan

[‡] Division of Science of Materials, Graduate School of Science and Technology, Kobe University, Kobe 657, Japan

Received 18 October 1996, in final form 21 February 1997

Abstract. Ionic conduction in $\text{ZrF}_4\text{--BaF}_2$ glass is investigated using normal-mode analysis (NMA). The origin of two distinct timescales observed in an earlier nuclear magnetic resonance (NMR) study (Y Kawamoto and J Fujiwara 1990 *Phys. Chem. Glasses* **31** 117) is considered. First, it is shown that the present NMA gives a result that is satisfactorily consistent with molecular dynamics (MD) simulations. This indicates that the NMA method could be successfully applied to the present topic, as well as providing added support to the MD result. The two methods give a consistent explanation for the origin of the NMR observation; the fact that there are two timescales is attributable to the difference in mobility between two classes of fluoride ions, i.e., bridging fluoride (BF) and non-bridging fluoride (NBF). The present NMA also provides information additional to that from the MD results. The difference in mobility between BF and NBF becomes significant only below the glass transition temperature T_g . Further analysis has been made to characterize the conduction mechanism more clearly, by the use of normal-mode excitations. The main finding is that an activation process becomes important for BF conduction below T_g , whereas no such process is observed for NBF.

1. Introduction

Since fluorozirconate glasses were discovered by Poulain *et al* [1] in 1975, these glasses have attracted considerable attention owing to their possible applications as device materials. Fluorozirconate glasses exhibit remarkably high ionic conductivity [2, 3], good optical transparency, and the ability to contain a large amount of additives, such as rare-earth ions, which are important for applications in optically active devices. Although the static structures of these glasses are rather well understood [4], the mechanism of the ionic conduction is not yet understood very well.

In the previous two articles of this series [5, 6], we have shown that: (1) the mobility of fluoride ions in the $\text{ZrF}_4\text{--BaF}_2$ glass exhibits two distinct timescales; and (2) the fact that two timescales are observed can be attributed to the difference in mobility between bridging and non-bridging fluoride ions, which are distinguished according to their local ionic environments. The former finding was achieved by means of ^{19}F nuclear magnetic resonance (NMR) measurements [5], and the latter explanation, which was first suggested by Angel *et al* [7], is confirmed by our extensive molecular dynamics (MD) simulations [6]. Although MD simulation is a powerful tool for investigating dynamic properties of condensed materials from a microscopic point of view, it often requires an extremely long computation time to obtain good statistical accuracy, particularly for materials which exhibit

slow dynamics, such as glasses. In fact, the calculations of diffusion coefficients in our previous MD study were incomplete at low temperatures.

In this study, we applied normal-mode analysis (NMA) to the present topic. NMA generally requires less computation time than MD simulations, because it uses only static information on the potential energy hypersurface in a multi-dimensional configuration space. The curvature of the hypersurface gives us very useful information on the dynamics of configuration points which transit from one potential minimum to the others. Thus it has been extensively used in the study of water systems [8], in which such transitions determine the long-time dynamics.

The standard NMA is carried out using inherent ionic configurations $\mathbf{q}_j(t)$ ($j = 1, \dots, N$) which are obtained by quenching the instantaneous ionic configurations $\mathbf{r}_j(t)$ ($j = 1, \dots, N$) into local minima of the potential hypersurface. With inherent configurations, all normal modes have real and positive frequencies. In addition to the standard NMA, efforts have been made to extend the NMA method using instantaneous configurations without involving the quenching process. With instantaneous configurations, some of the normal modes may have imaginary frequencies, indicating that those modes are unstable. We refer to normal modes obtained with inherent configurations as NMs, and to those obtained with instantaneous configurations as INMs. Recent studies [9] suggest that one can estimate the diffusion coefficient using the INM density of states, because the imaginary modes are closely connected with the diffusion. In this study, we evaluate the self-diffusion coefficients of fluoride ions with INMs, and perform also normal-mode excitations with the NMs.

The present study consists of the following two steps. We first examine the reliability of the NMA method for the present purposes, by comparing the results obtained from the INM analysis with those from the MD simulation. We then perform NM excitations to accumulate further insight into the mechanism of conduction in the $\text{ZrF}_4\text{-BaF}_2$ glass near the glass transition temperature T_g , which was not accessible using MD methods. By means of the first step, we can lend additional support to the previous MD result as well. The second step is the main concern of the present paper.

Table 1. Potential parameters used in the present simulation.

Ion	z	n	a (Å)
F	-1.0	8.0	1.237
Zr	+4.0	8.0	1.517
Ba	+2.0	8.0	1.854

2. Model

The model system treated in the present simulation is $50\text{ZrF}_4\cdot 50\text{BaF}_2$, since our NMR data are available for the same composition. We used the rigid-ion potential model, which is given by

$$U_{ij} = \frac{z_i z_j e^2}{r_{ij}} + \left(1 + \frac{z_i}{n_i} + \frac{z_j}{n_j} \right) b_{ij} \exp \frac{a_i + a_j - r_{ij}}{\rho} \quad (1)$$

where ze is the ionic charge, a and n are the potential parameters, r_{ij} is the interionic separation, and b_{ij} ($=0.19 \times 10^{-12}$ erg) and ρ ($=0.29$ Å) are constants. Potential models of this type have been widely used for simulating various ionic systems. The potential

parameters used in this study are identical to those of Boulard *et al* [10]. Those for like pairs are listed in table 1. The Lorentz–Berthelot combining rule was used for unlike pairs.

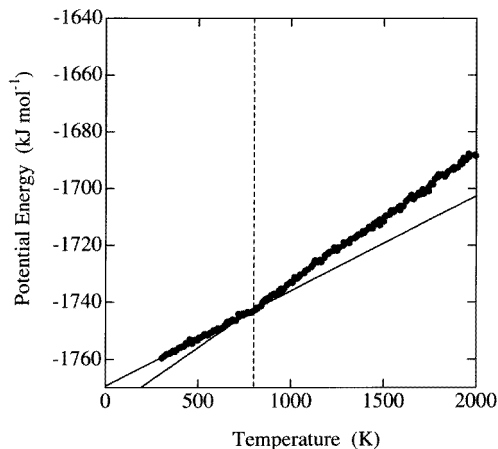


Figure 1. A plot of the total potential energy against decreasing temperature. T_g is observed near 800 K.

We first performed a constant-pressure MD simulation to estimate the glass transition temperature of the model system, by cooling the system continuously from 3000 K to 300 K. The cooling rate was -40 K ps^{-1} . The temporal total potential energies are plotted against temperature in figure 1. This plot shows a sharp bend near 800 K; this is T_g for the model system.

For a given ionic configuration, we put fluoride ions into two classes according to their local ionic environments. These are bridging fluoride ions (BF), which have two or more coordinating zirconium ions around them (Zr-F-Zr), and non-bridging fluoride ions (NBF), which have one or no coordinating zirconium ions around them (Zr-F-(Ba) , $(\text{Ba})\text{-F-(Ba)}$). The Zr coordination number was determined from the number of Zr ions within the first minimum in the partial radial distribution function $g_{\text{F-Zr}}(r)$.

3. Results

3.1. Instantaneous-normal-mode analysis

The standard technique for obtaining NMs is rather well known [11], and thus we do not repeat it here. For a given inherent atomic configuration which consists of N atoms ($3N$ degrees of freedom), one can obtain $3(N - 1)$ sets of phonon frequencies ω_i and eigenvectors \mathbf{V}_i by means of NMA (subscript i indicates the i th normal mode). INMs can be obtained by the same technique as that used to find NMs, but an instantaneous configuration is used. For a given instantaneous configuration, one obtains INMs as an output. The most important difference between NMs and INMs is that INMs may contain modes with imaginary frequencies (unstable modes), whereas NMs have only real and positive frequencies (stable modes). By calculating NMs (or INMs) with many ionic configurations at a given temperature and density, one can obtain NM (or INM) densities

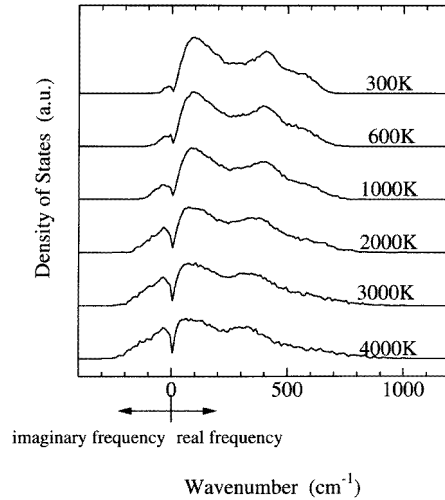


Figure 2. The INM densities of states at various temperatures. The imaginary parts are plotted in the negative direction.

of states (DOS) $\mathcal{D}(\omega)$ as follows:

$$\mathcal{D}(\omega) \equiv \left\langle \frac{1}{3N} \sum_{i=1}^{3N} \delta(\omega - \omega_i) \right\rangle \quad (2)$$

where $\langle \rangle$ denotes the ensemble average. Figure 2 shows the INM density of states of the model $\text{ZrF}_4\text{-BaF}_2$ glass at various temperatures. Imaginary parts of the DOS $\mathcal{D}_u(\omega)$ are plotted on the negative wavenumber axis for display purposes. Each curve is obtained by averaging the DOS over ten different configurations at a given temperature. One can observe that the area of the imaginary part increases with increasing temperature, reflecting the fact that the diffusion coefficient becomes larger with increasing temperature.

Contributions to the DOS from each ionic component X (=Ba, Zr, BF, NBF) can be obtained by adding a weighting parameter w_i^X to equation (2):

$$\mathcal{D}_X(\omega) \equiv \left\langle \frac{1}{3N} \sum_{i=1}^{3N} w_i^X \delta(\omega - \omega_i) \right\rangle \quad (3)$$

$$w_i^X \equiv \frac{\sum_j^{N_X} |v_i^j|^2}{\sum_j^N |v_i^j|^2} \quad (4)$$

where the summation $\sum_j^{N_X}$ runs over ionic component X only, v_i^j is the j th-ion part of the eigenvector \mathbf{V}_i ($\ni v_i^1, v_i^2, \dots, v_i^N$) of the i th mode, where N_X is the number of ionic components X. Figure 3 shows the INM density of states divided into the contributions for each X at 600 K and 3000 K.

In recent years, Keyes and co-workers have developed a novel approach for estimating the diffusion coefficients by use of INMs [9]. The advantage of their method is that it requires less computation time than the standard MD technique if the system exhibits slow dynamics, such as is the case for glasses or supercooled liquids. According to them, the self-diffusion coefficient D can be related to the INMs as follows:

$$D \sim f_u \overline{\omega_u} \quad (5)$$

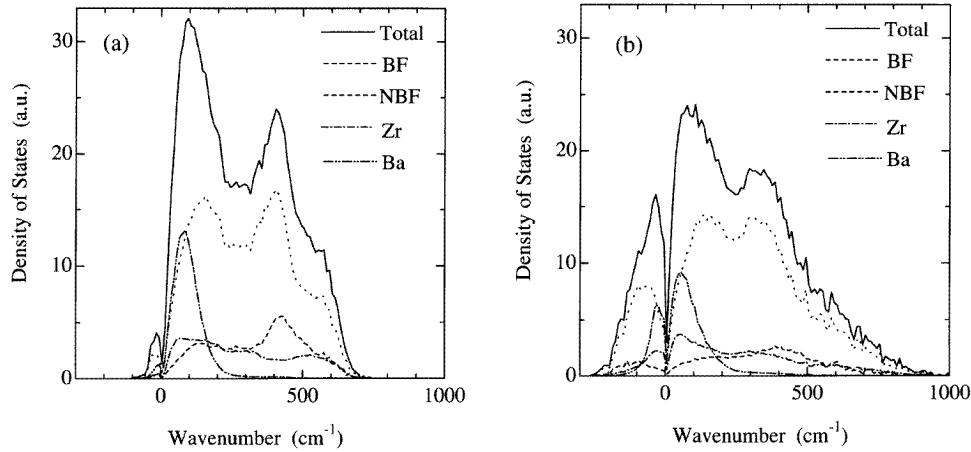


Figure 3. Contributions to the INM density of states from each of the ions at 600 K (a) and 3000 K (b).

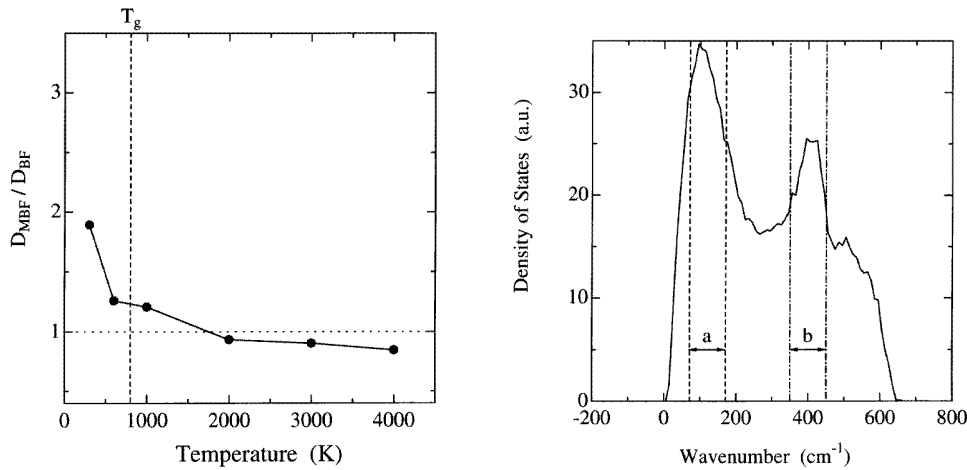


Figure 4. The ratio D_{NBF}/D_{BF} as a function of the temperature.

Figure 5. The NM density of states at 600 K.

where f_u is the area of $\mathcal{D}_u(\omega)$ normalized by the total area of $\mathcal{D}(\omega)$, and $\bar{\omega}_u$ is the average frequency of unstable modes. The diffusion coefficients were calculated separately for BF (D_{BF}) and NBF (D_{NBF}), according to equations (3) and (5). We plotted the ratio D_{NBF}/D_{BF} in figure 4. It is seen that D_{NBF}/D_{BF} is significant only below the glass transition temperature, whereas it approaches unity with increasing temperature. The change in D_{NBF}/D_{BF} at around T_g is sharp. This suggests that the conduction mechanism of either BF or NBF changes at around T_g .

3.2. Normal-mode excitation

Below T_g , the ionic diffusion can be understood as a sequence of ionic jump motions, i.e., a transition from one inherent configuration to the others on the multi-dimensional

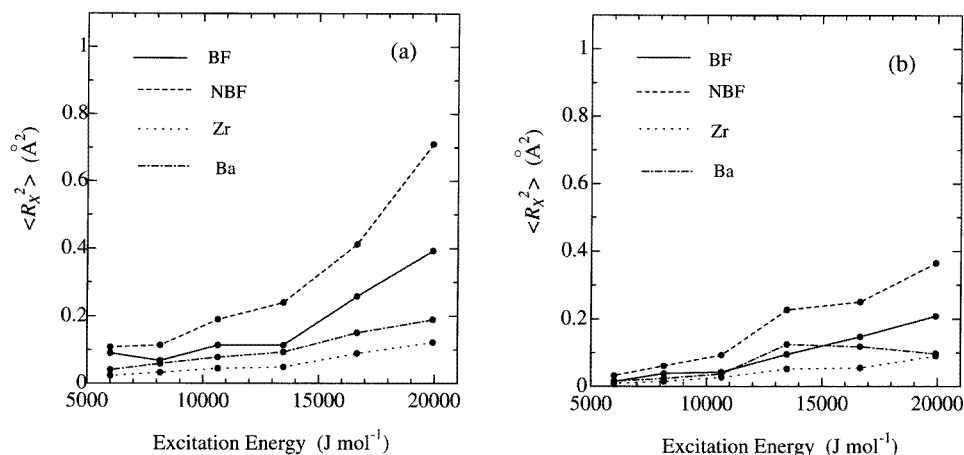


Figure 6. The mean square displacements (R_X^2) after NM excitations with various kinetic energies. The starting configurations were obtained from MD simulations at 600 K, and the excitations were for the frequency ranges 70–170 cm^{-1} (a) and 350–450 cm^{-1} (b).

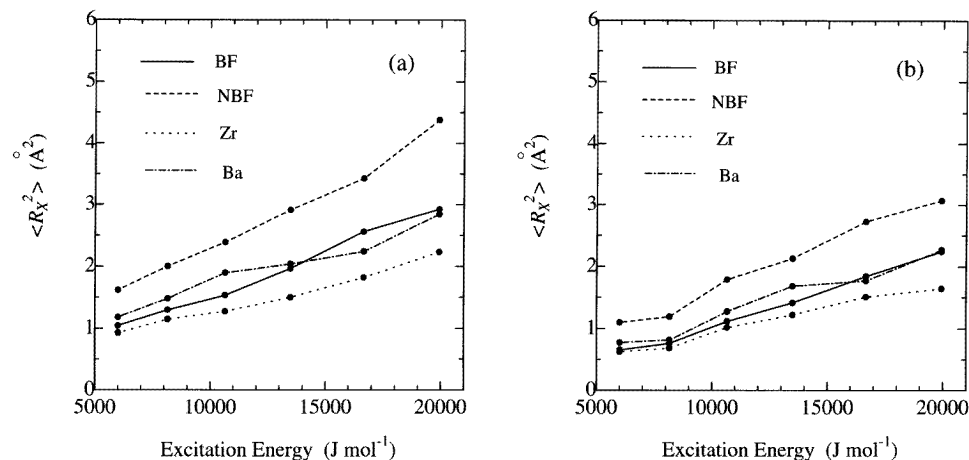


Figure 7. The mean square displacements (R_X^2) after NM excitations with various kinetic energies. The starting configurations were obtained from MD simulations at 4000 K, and the excitations were for the frequency ranges 70–170 cm^{-1} (a) and 350–450 cm^{-1} (b).

potential hypersurface. It is thus meaningful to perform trajectory calculations starting from an inherent configuration by exciting some NMs. This technique is called the normal-mode excitations (NME) method. We performed the NME method at 600 K (below T_g) and at 4000 K (above T_g) in the following manner.

- (1) The starting instantaneous ionic configurations $r_j(t)$ were obtained by performing standard constant-pressure–temperature MD simulations at 600 K or 4000 K.
- (2) The inherent ionic configurations $q_j(t)$ were obtained by quenching the instantaneous configurations $r_j(t)$, and then the NMs were calculated.
- (3) Ten NMs were chosen randomly from the frequency range 70–170 cm^{-1} , which corresponds to the main peak (a) in the NM density of states, as shown in figure 5.

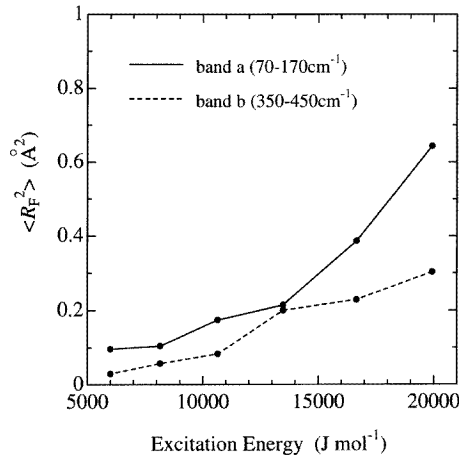


Figure 8. A comparison of the mean square displacement obtained by exciting the range a (70–170 cm^{-1}) and the range b (350–450 cm^{-1}).

(4) These NMs were excited simultaneously. Equal energies were given to each selected NM. Excitations with six different total energies were performed.

(5) Trajectory calculations were performed by means of constant-energy MD simulations over a time interval of $\Delta t = 10$ ps, and final instantaneous configurations $r_j(t + \Delta t)$ were obtained.

(6) The final inherent configurations $q_j(t + \Delta t)$ were obtained by quenching $r_j(t + \Delta t)$.

We performed the above trajectory calculation for ten different starting configurations at a given temperature, and measured the mean square displacement

$$\langle R_X^2 \rangle \equiv \left\langle \frac{1}{N_X} \sum_j^{N_X} (q_j(t + \Delta t) - q_j(t))^2 \right\rangle \quad (6)$$

for each ionic component X. These are plotted in figures 6(a) and 7(a). The following features are found.

(1) Both above and below T_g , the displacements are larger for NBF than for BF over the whole energy range considered in this paper.

(2) Above T_g , all of the ions show large displacements, and the displacement increases monotonically with increasing excitation energy. This indicates that all of the ions are freely mobile above T_g .

(3) Below T_g , the displacements of the BF are almost of the same order as those of Ba and Zr, which are not conductive, if the excitation energy is smaller than 13 500 J mol^{-1} . BF is conductive only if the excitation energy exceeds 13 500 J mol^{-1} , whereas NBF is mobile over the whole energy range considered. This indicates that there is a certain activation process for BF conduction below T_g . This activation process could be the origin of the sharp increase in the difference in mobility between BF and NBF below T_g .

Excitations within the frequency range 350–450 cm^{-1} , which corresponds to the second peak (b) in the NM density of states, were also made. These are plotted in figure 6(b) and 7(b). The trends observed are almost the same as those seen for the 70–170 cm^{-1} band excitations. By comparing figure 6(a) with figure 6(b), one finds that the displacements

obtained with range-b excitations are always smaller than those obtained with range-a excitations if the total excitation energies are equal. This is more clearly shown in figure 8, in which the displacements of the total fluoride ion (BF+NBF) at 600 K are plotted separately for range-a and range-b excitations. This plot suggests that lower-frequency phonons give a greater contribution to the ionic diffusion than those of higher frequency.

4. Discussions

Although some efforts to apply the NMA method to a study of glass systems have already been made [12], they have been carried out using simple potential models only. To the best of our knowledge, this is the first attempt in which there has been a successful application of the NMA to a study of ionic conduction in glasses, using a realistic potential model. In this section, we briefly review our previous MD simulation, and discuss the advantages of the NMA method over the conventional MD method.

We performed extensive MD simulations for the same glass material as was examined in the previous study [6], in order to improve on the earlier MD results [7]. Simulations were carried out at temperatures of 1000 K and 4000 K, which correspond to glass and molten states, respectively [13]. At higher temperature, we were able to successfully calculate the diffusion coefficients of the two classes of fluoride ions separately, by the use of the first-passage-time approach (FPTA) [14]. However, we could not apply the FPTA at lower temperature, because the ion jumps happen only very rarely, even in our long-time simulation (10 ns = 2 000 000 MD steps). Instead of calculating the diffusion coefficient by means of the FPTA, we calculated the average departure distance r_1 for a time interval of 9 ns for BF and NBF from the self-part of the van Hove correlation function. The distance r_1 should be proportional to the diffusion coefficient. By comparing r_1 for BF with that for NBF, we estimated that $D_{\text{NBF}}/D_{\text{BF}}$ is about 2 below T_g . This result is consistent with the present NMA result, which also gives a value of $D_{\text{NBF}}/D_{\text{BF}}$ of about 2 below T_g (see figure 4; one finds that MD simulation and NMA can give the same result, at least qualitatively). We believe that this agreement indicates that the NMA is a reliable method for investigating the ionic conduction dynamics in glass materials. It should be noted that MD simulation requires 2 000 000 time-integration steps to obtain this result, but the NMA requires a computation time which corresponds approximately to 200 000 MD steps for each run. Thus we were able to perform ten independent runs to reduce the statistical errors by using NMA in this study, where only one MD run could have been done in the previous work. This means that the NMA method is possibly about ten times more efficient than conventional MD simulation methods for studying the dynamics of glass materials.

5. Concluding remarks

In the previous two articles of this series, we have shown that: (1) the mobility of fluoride ions in the $\text{ZrF}_4\text{-BaF}_2$ glass has two distinct timescales; and (2) the two timescales observed can be attributed to the difference in mobility between bridging and non-bridging fluoride ions, which are defined according to their local ionic environments. In this study, we applied normal-mode analysis (NMA) to the present topic because it requires, in general, less computation time than MD simulation for obtaining the same information. We have used the INM formalism recently developed by Keyes and co-workers to compare the mobility of BF and NBF, and subsequently to examine the reliability of the NMA method by comparing the present results with the previous MD results. The results obtained by

the two methods were satisfactorily consistent. These facts clearly indicate that NBF is more mobile than BF below T_g , whereas the difference in mobility becomes small above T_g . In addition to confirming the MD result, the present NMA has added new information as well. A sharp change in the mobility difference at around T_g was found. This behaviour could not be observed in the previous MD simulations. We believe that this is because of the insufficient MD simulation time allowed, since MD simulation requires very long computation times when the system nears the glass transition.

We have also performed normal-mode excitations below (at 600 K) and above (at 4000 K) T_g to accumulate further insight into the conduction mechanism of the $\text{ZrF}_4\text{-BaF}_2$ glass near T_g . The mean square displacements after the excitations with different excitation energies were calculated and plotted. No significant qualitative differences were found among the ionic components above T_g . We observed the following important features below T_g . (1) The displacements are larger for NBF than for BF over the whole energy range considered in this paper. (2) BF is mobile only if the excitation energy exceeds $13\,500\text{ J mol}^{-1}$, whereas NBF is mobile over the whole energy range considered. This indicates that a certain activation process becomes important for BF conduction below T_g . We believe that the sharp increase in the mobility difference between BF and NBF observed below T_g is attributable to this activation process. These trends were observed both with $70\text{--}170\text{ cm}^{-1}$ and with $350\text{--}450\text{ cm}^{-1}$ band excitations. It was also found that the displacements with $350\text{--}450\text{ cm}^{-1}$ band excitations are smaller than those with $70\text{--}170\text{ cm}^{-1}$ band excitations. This suggests that the lower-frequency band gives a greater contribution to the ionic diffusion.

In the course of the present study, we were able to conclude that the NMA method can give useful information in less computation time than is required for the corresponding MD simulation in the investigation of ionic conduction dynamics at lower temperatures, particularly below T_g .

Acknowledgments

The authors thank Dr H Tanaka for fruitful discussions. They also thank Professor Y Kawamura for providing the original MD code used in the present study. This work was supported by a Grant in Aid for Scientific Research from the Ministry of Education, Science and Culture. The calculations were carried out at the Supercomputer Laboratory, Institute for Chemical Research, Kyoto University, and the Computer Centre of the Institute for Molecular Science, Okazaki, Japan.

References

- [1] Poulain M, Poulain M and Lucas J 1975 *Mater. Res. Bull.* **10** 243
- [2] Leroy D, Lucas J, Poulain M and Ravaine D 1978 *Mater. Res. Bull.* **13** 1125
- [3] Ravaine D and Leroy D 1980 *J. Non-Cryst. Solids* **38+39** 575
- [4] Kawamoto Y, Horisaka H, Hirao K and Soga N 1985 *J. Chem. Phys.* **83** 2398
- [5] Kawamoto Y and Fujiwara J 1990 *Phys. Chem. Glasses* **31** 117
- [6] Yamamoto R, Kobayashi T and Kawamoto Y 1995 *J. Phys.: Condens. Matter* **7** 8557
- [7] Angel C A, Cheeseman P A and Tamaddon S 1982 *J. Physique Coll.* **43** C9 381
- [8] Ohmine I and Tanaka H 1993 *Chem. Rev.* **93** 2545
- [9] Madan B, Keyes T and Seeley G 1990 *J. Chem. Phys.* **92** 7565
Madan B, Keyes T and Seeley G 1991 *J. Chem. Phys.* **94** 6762
Madan B and Keyes T 1993 *J. Chem. Phys.* **98** 3342
Moore P and Keyes T 1994 *J. Chem. Phys.* **100** 6709
- [10] Boulard B, Kieffer J, Phifer C C and Angel C A 1992 *J. Non-Cryst. Solids* **140** 350

- [11] Goldstein H 1981 *Classical Mechanics* (Reading, MA: Addison-Wesley) ch 6
- [12] Bembenek S D and Laird B B 1995 *Phys. Rev. Lett.* **74** 936
- [13] The glass transition temperature of the model $\text{ZrF}_4\text{-BrF}_2$ glass used in the previous MD study is near 1200 K, because we used another set of potential parameters in formulating it. In the present study, we used a set of potential parameters proposed by Boulard *et al* which is believed to be more reliable for the present system.
- [14] Munakata T and Kaneko Y 1993 *Phys. Rev. B* **47** 4076